Gas Quantification Using Arrays of Intrinsic Zinc Oxide Thin Films Fabricated Using Three Different Successive Ionic Layer Adhesion and Reaction Processes

AMALLA, Bon Leif D.

February 14, 2019

Contents

List of Figures iii

List of Figures iv

1 Introduction 1

1.1 Background of the Study . . . 1

1.2 Objectives of the Study . . . 3

1.3 Significance of the Study . . . 3

1.4 Scope and Limitations . . . 4

2 Review of Related Literature 5

2.1 Zinc oxide . . . 5

2.1.1 Crystal structure . . . 5

2.1.2 Electrical properties . . . 6

2.1.3 Successive ionic layer adhesion and reaction processes . . . 7

2.2 Multiscale Modeling . . . 9

2.2.1 Representative volume elements . . . 9

2.2.2 Finite element methods . . . 9

2.2.3 Deep learning methods . . . 9

2.2.4 Property localization . . . 9

2.2.5 Property homogenization . . . 9

2.3 Materials knowledge systems . . . 9
2.3.1 Microstructure functions . . . 9
2.3.2 One-point spatial correlations . . . 9
2.3.3 Two-point spatial correlations . . . 9
2.4 Julia . . . 10
2.4.1 Comparison with currently used languages . . . 10
2.4.2 Language features . . . 10
2.4.3 Syntax . . . 10
2.4.4 Published computational studies and applications . . . 10

3 Methodology **11**
3.1 Thin Film Fabrication . . . 11
3.2 Thin Film Characterization . . . 12
3.3 Model Creation . . . 13
3.3.1 Definition of microstructure functions . . . 13
3.3.2 Calculation of two-point spatial correlations . . . 13
3.3.3 Determination of optimal film orientation . . . 15
3.3.4 Determination of optimal microstructure function . . . 15

References **16**

List of Tables

3.1 Processing parameters manipulated and SILAR processes 11

3.2 Summary of discrete microstructure functions 14

List of Figures

3.1 Basic orientation matrix 12

3.2 Four point probe mechanism for determination of sheet resistance 12

Chapter 1

Introduction

1.1 Background of the Study

Zinc oxide is a metal oxide semiconductor that has many different uses based on its structure such as in thin film electronics. Zinc oxide thin films are used in a wide variety of applications as gas sensors (Florido & Dagaas, 2017) and as photovoltaic cells (Saikumar, Skaria, & Sundaram, 2014). In order for the material to perform predictably, it is necessary to be able to correlate processing parameters to structural characteristics and property manifestations (Florido & Dagaas, 2017; Saikumar et al., 2014).

Due to the promise of rapid, high-throughput materials processing brought by data science driven approaches to materials processing through materials knowledge systems (MKS) frameworks (Gupta, Cecen, Goyal, Singh, & Kalidindi, 2015; Sun, Cecen, Gibbs, Kalidindi, & Voorhees, 2017; Yabansu, Patel, & Kalidindi, 2014) the field of materials informatics has grown.

There are several studies on computational simulations regarding material properties based on material structure and vice versa (Gupta et al., 2015; Yabansu et al., 2014).

The MKS framework, as defined by Yabansu et al. (2014), is dependent on the definition of a microstructure function m_r^n, representing the probability density of finding a specific local state $n \in N$, characterized by physical and chemical properties, at a spatial bin $r \in R$. A number of studies have proposed the MKS to use discretized microstructure functions in order to apply statistical measures (Gupta et al., 2015; Sun et al., 2017; Yabansu et al., 2014). Numerous studies regarding the use of MKS frameworks have produced different microstructure functions depending on the application of the materials of interest ranging from two to ten and more local states (Gupta et al., 2015; Sun et al., 2017; Yabansu et al., 2014).

Property homogenization, within a probe volume, can be easily achieved through calculation and regression of calculated two point spatial correlations derived from assumptions of periodicity of the microstructure function in a given probe volume V. Research done by Sun et al. (2017) has shown that the assumption of periodicity of the microstructure function in a probe volume can make drastic computational improvements to the MKS compared to using finite element methods.

Currently, there exists an implementation of the MKS framework in the Python programming language (PyMKS) (Wheeler, Brough, Fast, Kalidindi, & Reid, 2014). The said framework implementation is maintained by researchers Georgia Institute of Technology and has been developed by a number of contributors to the repository. It is currently available on Github as an open-source project licensed under the MIT license.

As a rapidly growing computational language, Julia has proven to be more efficient and effective as other computational programming languages such as Matlab, Python (NumPy), and Octave (Bezanson, Edelman, S., & Shah, 2015). Examples of scientific applications are as a simulator for different systems dynamics through BioSimulator.jl (Landeros et al., 2018), for different quantum systems through QuantumOptics.jl (Krämer, Plankensteiner, Ostermann, & Ritsch, 2018), and modeling protein electrostatics using finite element methods through NESSie.jl (Kemmer, Rjasanow, & Hildebrandt, 2018).

1.2 Objectives of the Study

The study aims to be able to define a new, simple microstructure function for the effective creation of MKS in developing material PSP linkages for the distribution of adhered particles of zinc oxide onto glass substrates. Specifically, the study will attempt to cover and discuss necessary measures that will aid in the creation of effective discrete spatial statistics of the particles, particle boundaries, and null spaces within the material structure, which will be used to find correlations to manipulations in the number of deposition cycles and annealing temperature.

The study also aims to be able to create a MKS methodology template in the Julia programming language. Specifically, the study aims to provide a new platform for materials informatics using the features of the programming language.

1.3 Significance of the Study

Some of the numerous applications of zinc oxide thin films are dependent on the different distribution-dependent properties of the material, including thin film sheet resistance, porosity, and transmittance. The computational modeling of zinc oxide material structure with respect to processing parameters and properties is a significant milestone for the rapid, high-throughput production of precise application-specific materials.

The expression of the MKS framework, case-dependent or independent, in multiple languages allows for the growth of the framework into several applications allowing open source communities to further develop the capabilities of the framework.

1.4 Scope and Limitations

The study mainly focuses on determining a family of microstructure functions that can be useful for building PSP linkages given sufficient material characterization. Since characterization is not readily accessible, structural characteristics used may be of low resolution. Thus, heavy caution must be observed in interpreting the results of the study.

Chapter 2

Review of Related Literature

2.1 Zinc oxide

2.1.1 Crystal structure

One of the key characteristics governing most of the properties of condensed matter is the crystal structure of a material. The crystal structure is thus important in characterizing material.

Zinc oxide is a metal oxide semiconductor having a hexagonal crystal structure. In studies such as those of Gao, Li, and Yu (2004) and Rajkumar et al. (2015), there are three identified main peaks in the diffaction pattern (see Characterization Methods) of zinc oxide. These three peaks are the first three peaks in the diffraction pattern of ZnO found roughly at $2\theta \in \{32^\circ, 34^\circ, 36^\circ\}$. The planes of diffraction are (100), (002), and (101), respectively, with the highest peaks at the (002) plane suggesting preferrential orientation in the c-axis. With regard to flat surfaces, this suggests formation of vertical rod-like structures from the substrates.

Numerous studies such as those of Gao et al. (2004), Vargas-Hernández, Jiménez-García, Jurado, and Henao Granada (2008a), and Rajkumar et al. (2015) have shown experimentally that this structure of zinc oxide can be achieved even through production using different processes. All of these showed that manipulating the processing parameters have various effects on the crystalline structure of the material. They have effects on the crystallite size and relative intensities (diffraction). It is worth noting that the processes used for fabrication are SILAR processes, as will be described in a later section.

The three SILAR processes analyzed by Vargas-Hernández et al. (2008a) showed differences in the relative intensities of the diffraction peaks. It can also be noted that some of the diffraction peaks present in films fabricated by a process were not found in another. Rajkumar et al. (2015) showed how different doping concentrations affected the overall crystallinity of the thin film structure. The results, as expected, showed that different processing parameters lead to different material crystal structures.

2.1.2 Electrical properties

Studies have shown that zinc oxide thin films exhibit a wide variety of interesting properties such as *band gap* and *electrical resistivity*. Those of Rajkumar et al. (2015) and Vargas-Hernández et al. (2008a) made empirical studies on the effects of different processes on the electrical properties of ZnO. Specifically, Rajkumar et al. (2015) compared band gaps and electrical resistivity, while Vargas-Hernández et al. (2008a) compared band gap. Just as different processing parameters have led to differences in material crystal structures, the difference in crys

Research on zinc oxide thin films as gas sensors by exploiting the reversible reactions of reducing gases to the surface of the material (Florido & Dagaas, 2017). These surface reactions change the movement of charges within the crystal structures of materials affecting their *resistivity*. There is more literature that shows how crystal structures affect the electrical resistivity and gas sensing response of metal oxide semiconductors from theoretical studies such as of Dey (2018) and Hua et al. (2018) to *in silica* studies like involving DFT (Zhao et al., 2013); however, these will not be focused on in this study.

The importance of being able to computationally predict the properties similar to the *in silica* study referred to above is a huge milestone in predicting properties given the structure of a material.

2.1.3 Successive ionic layer adhesion and reaction processes

Successive ionic layer adhesion and reaction (SILAR) processes are a family of processes wherein materials are deposited onto substrates by means of successive surface reactions. The processes described will be based on the study by Gao et al. (2004).

The processes consist of two main phases: a *deposition* phase and an *annealing* phase. The deposition phase in material fabrication involves a set of precursor solutions: cationic solutions, complexing solutions, and anionic solutions, to perform the reactions on the surface of the substrate. The three solutions are aqueous (Gao et al., 2004). Thus, the substrate surface must be hydrophilic for the solutions to react in the and adhere. However, naturally, glass is hydrophobic which can be noted by the formation of droplets on its surface. Gao et al. (2004) suggested the following methodology to develop the hydrophilic property of glass surface: boil the substrates in dilute H_2SO_4 (1 : 10 v/v) for 30 minutes, then completely rinse the substrates in ethanol, acetone, and de-ionized water. Similar processes were also done by Rajkumar et al. (2015) and Vargas-Hernández et al. (2008a).

A study conducted by Vargas-Hernández, Jiménez-García, Jurado, and Henao Granada (2008b) was performed in order to determine the effects of three different number of deposition cycles to thin film crystallinity. It was observed that the relative intensities of the diffraction peaks drastically increased with the number of deposition cycles. However, there was no literature, as of this manuscript, that can be used to explain this phenomenon. It should be noted that the studies conducted by Vargas-Hernández et al. (2008b) and Vargas-Hernández et al. (2008a) differ in the parameter tested in SILAR processing.

In addition to the precursor solutions and substrate properties described, another factor that affects the output of SILAR processes is the drying interval being deployed between each dipping processes (Gao et al., 2004). In the cited literature, the researchers compared the effects of two drying processes in the crystallinity of the thin films. In applying a drying process of $3-5$ or 30 seconds between each deposition *cycle*, the resulting thin films have a defined and *periodic* microstructure. Those films processed with no drying process between each deposition cycle were found to have *amorphous* microstructures.

The annealing process in SILAR processes is crucial for the growth of crystal structures in the thin film. According to Rajkumar et al. (2015), it is still unknown how, specifically, annealing affects this growth. There are numerous *empirical* studies regarding this topic, however, there is currently no solid theory known to the researchers as of date.

In the study of Rajkumar et al. (2015), it can be observed through the XRD spectra that annealing plays a huge role in the development of crystal structures. It can be seen that the measured intensities at the Bragg angles stated above have increased. This means that better crystallinity is achieved through thermal annealing. The study of Gao et al. (2004) has found that there can also be different effects on thin film crystallinity based on the annealing environment used. It can be inferred from the data that the adjusting the annealing environment leads to different average crystallite sizes within the thin films.

Studies by Vargas-Hernández et al. (2008a), Vargas-Hernández et al. (2008b), Gao et al. (2004), and Rajkumar et al. (2015) all have used different precursor solutions in preparing thin films.

2.2 Multiscale Modeling

2.2.1 Representative volume elements

2.2.2 Finite element methods

2.2.3 Deep learning methods

2.2.4 Property localization

2.2.5 Property homogenization

2.3 Materials knowledge systems

2.3.1 Microstructure functions

2.3.2 One-point spatial correlations

2.3.3 Two-point spatial correlations

Calculation of values

Low dimensional space representation

Principal component analysis

Partial least squares analysis

2.4 Julia

2.4.1 Comparison with currently used languages

2.4.2 Language features

Data representation

Data types

Multiple dispatch

Parallel programming

2.4.3 Syntax

Function representation

Mathematical representation

2.4.4 Published computational studies and applications

NESSie.jl

JuMP.jl

BioSimulator.jl

QuantumOptics.jl

Chapter 3

Methodology

3.1 Thin Film Fabrication

Thirty glass substrates, measuring 1” $\times$ 0.25”, were cut from microscope slides. These substrates were subject to three successive ionic layer adhesion and reaction (SILAR) processes, S1, S2, and S3, as will be detailed in this section. All of the SILAR processes consist of a certain number of deposition cycles from a fixed precursor solution with $0.095M$ Zn^{2+} and $0.190M$ NaOH and a thermal annealing at certain temperatures (Florido & Dagaas, 2017; Gao et al., 2004).

Table 3.1 summarizes the different SILAR processes along with the variations in processing parameters.

Table 3.1: Processing parameters manipulated and SILAR processes

—	S1	S2	S3
Depostion cycles	100	75	100
Annealing temperature	450°C	450°C	500°C

1	3
2	4

Figure 3.1: Basic orientation matrix

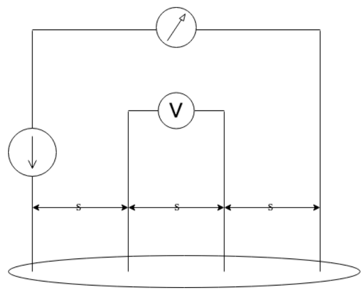

Figure 3.2: Four point probe mechanism for determination of sheet resistance

3.2 Thin Film Characterization

The fabricated thin films were characterized for determination of thin film structure and properties.

One thin film fabricated using each of the fabrication processes was chosen for optical microscopy. The fabricated material was split into four sections as shown in Figure 3.1. The sections were chosen such that the four corners of the rectangular substrate represent different probe volumes. The thin films were viewed under the high power objective lens (400×) of a digital compound microscope.

Overall thin film structure were also characterized with x-ray diffraction, using Cu-Kα anode ($\lambda = 1.54\,\text{Å}$), and scanning electron microscopy at 20 kV.

Finally, the thin films sheet resistance values were derived from measurements from four-point probe sensing. The schematic for the four-point probe mechanism are shown in Figure 3.2.

3.3 Model Creation

3.3.1 Definition of microstructure functions

There are a total of 20 discrete microstructure functions (DMF) that are studied for the study. The definitions are divided into four categories depending on which of two axes will the DMFs be assumed to be periodic in. Each of the four categories contains five DMFs, which differ based on the method for determining the number of discrete local states within a certain probe volume V.

The functions can be summarized as Table 3.2. The dimensions of the probe volume V were chosen as odd products of small primes (2, 3, 5, and 7) to aid in the computation of two point spatial correlations, as will be discussed in the following subsection, with the exception of one function, with accounts for the dimensions of the size of a high resolution digital image.

3.3.2 Calculation of two-point spatial correlations

Two point spatial correlations are derived from optical microscopy images through the definition of the measures (Gupta et al., 2015).

$$m_r^{np} = \frac{1}{S_r N} \sum_{i=0}^{N} \sum_{i=0}^{R} m_r^p m_r^n$$

where n, p are the discrete local states of interest and r is the spatial bin of interest.

Image data were transformed into Julia 2D arrays (Bezanson et al., 2015) and further into a user defined data structure named *MaterialImage* which accounts for the parameters used for defining the DMFs (from the previous subsection). There are a total of 20 sets two point spatial correlations that will be considered.

Table 3.2: Summary of discrete microstructure functions

Periodic axes	Local states	Size of V
Both i, j	Two	225×225
Both i, j	Two	441×441
Both i, j	Three	225×225
Both i, j	Three	441×441
Both i, j	Three	1920×1080
j	Two	225×225
j	Two	441×441
j	Three	225×225
j	Three	441×441
j	Three	1920×1080
i	Two	225×225
i	Two	441×441
i	Three	225×225
i	Three	441×441
i	Three	1920×1080
None	Two	225×225
None	Two	441×441
None	Three	225×225
None	Three	441×441
None	Three	1920×1080

3.3.3 Determination of optimal film orientation

Since the preferred orientation of the fabrication of thin films is unknown, each of the three thin films have four hypothesized orientations based on circular permuations of the orientation matrix (Figure 3.1).

For each of the calculated two point spatial correlations, the values will undergo principal component analysis to obtain the orthogonal latent descriptors (Gupta et al., 2015; Sun et al., 2017). This is done with *MultivariateStats.jl*, a package available for multivariate statistical analysis (Dahua, 2018). Optimal orientation is determined when the variance of the dimensionally-reduced two point statistics, *i.e. the matrix trace of the covariance matrix* is minimized.

3.3.4 Determination of optimal microstructure function

The plots for the two-point statistics are manually compared. Partial least squares analysis (PLSA) is done to compare the ability of the DMF to capture the variation of derived sheet resistance values. Evaluation of the optimal microstructure function will be based on the following parameters:

1. Variance capture via PLSA

2. Qualitative assessment of clustering of microstructure ensembles

References

Bezanson, J., Edelman, A., S., K., & Shah, V. B. (2015). Julia: A fresh approach to numerical computing. *Society for Industrial and Applied Mathematics*, *59*, 65–98.

Dahua, L. (2018). Multivariatestats documentation [Computer software manual]. Retrieved 24 Jan 2018, from `media.readthedocs.org/pdf/multivariatestatsjl/latest/multivariatestatsjl.pdf`

Dey, A. (2018). Semiconductor metal oxide gas sensors: A review. *Materials Science and Engineering B*, *229*, 206–217.

Florido, E. A., & Dagaas, N. A. C. (2017). Carbon monoxide gas sensing using zinc oxide deposited by successive ionic layer adhesion and reaction. *IOP Conf. Series: Materials Science and Engineering*, *201*.

Gao, X. D., Li, X. M., & Yu, W. D. (2004). Synthesis and optical properties of ZnO nanocluster porous films deposited by modified SILAR method. *Applied Surface Science*, *229*, 275–281.

Gupta, A., Cecen, A., Goyal, S., Singh, A. K., & Kalidindi, S. R. (2015). Structure-property linkages using a data science approach: Application to a non-metallic inclusion/steel composite system. *Acta Materialia*, *91*, 239–254.

Hua, Z., Tian, C., Huang, D., Yuan, W., Zhang, C., Tian, X., … Li, E. (2018). Power-law response of metal oxide semiconductor gas sensors to oxygen in presence of reducing gases. *Sensors and Actuators B: Chemical*, *267*, 510–518.

Kemmer, T., Rjasanow, S., & Hildebrandt, A. (2018). NESSie.jl: Efficient and intuitive finite element and boundary element methods for nonlocal protein electrostatics in the Julia language. *Journal of Computational Science*, *28*, 193–203.

Krämer, S., Plankensteiner, D., Ostermann, L., & Ritsch, H. (2018). QuantumOptics.jl: A Julia framework for simulating open quantum systems. *Computer Physics Communications*, *227*, 109–116.

Landeros, A., Stutz, T., Keys, K. L., Alekseyenko, A., Sinsheimer, J. S., Lange, K., & Sehl, M. E. (2018). Biosimulator.jl: Stochastic simulation in Julia. *Computer Programs and Methods in Biomedicine*, *167*, 23–35.

Rajkumar, P. V., Ravinandran, K., M., B., Ravidhas, C., B., S., & Dineshbabu, N. (2015). Enhancement of optical and electrical properties of SILAR deposited ZnO thin films through fluorine doping and vacuum annealing for photovoltaic applications. *Materials Science in Semiconductor Processing*, *35*, 189–196.

Saikumar, A. K., Skaria, G., & Sundaram, K. B. (2014). ZnO gate based MOSFETs for sensor applications. *ECS Transactions*, *61*, 65–69.

Sun, Y., Cecen, A., Gibbs, J. W., Kalidindi, S. R., & Voorhees, P. W. (2017). Analytics on large microstructure datasets using two-point spatial correlations: Coarsening of dendritic structures. *Acta Materialia*, *132*, 374–388.

Vargas-Hernández, C., Jiménez-García, F. N., Jurado, J. F., & Henao Granada, V. (2008a). Comparison of ZnO thin films deposited by three different SILAR processes. *Microelectronics Journal*, *39*, 1349–1350.

Vargas-Hernández, C., Jiménez-García, F. N., Jurado, J. F., & Henao Granada, V. (2008b). XRD, μ-Raman and optical absorption investigations of ZnO deposited by SILAR method. *Microelectronics Journal*, *39*, 1347–1348.

Wheeler, D., Brough, D., Fast, T., Kalidindi, S., & Reid, A. (2014). *Pymks: Materials knowledge system in Python.*

Yabansu, Y. C., Patel, D. K., & Kalidindi, S. R. (2014). Calibrated localization relationships for elastic response of polycrystalline aggregates. *Acta Materialia*, *81*, 151–160.

Zhao, L., Tian, F., Wang, X., Zhao, W., Fu, A., Shen, Y., … Yu, S. (2013). Mechanism of CO absorption on hexagonal WO_3 (001) surface for gas sensing: A DFT study. *Computational Materials Science*, *79*, 691–697.